THE BELL SYSTEM TECHNICAL JOURNAL
Vol. 57, No. 9, November 1978
Printed in U.S.A.

Caustic Patterns Associated With Melt Zones in Solidified Glass Samples—Part I: Symmetric Cases

By T. D. DUDDERAR, J. B. SEERY, and P. G. SIMPKINS

(Manuscript received March 17, 1978)

Ray-tracing algorithms have been developed to follow the propagation of a collimated beam of light traveling along and refracting out of a glass rod in a region of monotonically decreasing cross section. These algorithms have been used to study the formation and distribution of caustics as a function of the changing cross-section area. Axial profile data taken from the melt, or drawdown, zone of a solidified fiber-drawing sample provide the geometrical information needed to predict the loci of two major and two minor families of caustics. General principles for relating the observable far-field caustic patterns to the actual shapes of symmetric melt zones in glass samples are discussed.

I. INTRODUCTION

When a plane light wavefront propagates along a cylindrical glass rod in which a rapid monotonic decrease in cross section occurs, some light may be refracted from the glass and become externally visible. For a sample with homogeneous optical properties, the amount of emerging light and its intensity distribution are strongly influenced by the rate at which the cross section decreases. In a previous study of melt, or drawdown, zones of solidified samples taken from a laser-heated fiber-drawing system, the boundaries between the regions of emitted light and shadow were seen to be loci of intense illumination properly identified as "caustics."[1] These caustics were shown, by both experiment and analysis, to arise from various internal reflections and a refraction of the light from the surface. It was noted that the number of caustics increases as the rate of change of the cross section increases. No light is emitted from a very gradually tapered sample, while a great deal of light and numerous caustics are emitted from a sample with a very rapid taper. Also, as the rate of change of the cross section increases, the propagation

vectors of the light rays which form the far-field caustic patterns rotate; i.e., from the pulling or downstream direction through the radial and toward the upstream direction.

During the initial investigation, ray-tracing algorithms were developed that permitted accurate calculation of the light paths necessary to identify the two principal caustics experimentally observed. These routines utilize actual melt zone profile data and polynomial spline-fitting procedures to provide the geometrical information necessary to describe the caustics for a given value of the index of refraction n. Experimental results from four radically different samples compared very favorably with those obtained from the algorithm within the limitations of the accuracy of the profile data itself.

The present study uses the algorithms to investigate the detailed response of the caustic loci to systematic changes in the melt zone geometry. Only rotationally symmetric homogeneous examples were considered. Results were obtained for a far greater range of melt zone tapers than were originally investigated experimentally.

II. PROCEDURE

None of the four samples discussed in the earlier reports was in fact rotationally symmetric. Three were specifically selected because of their existing asymmetries. It was found that, for certain cases, these geometric asymmetries influenced the far-field caustic patterns quite strongly. In the present study, symmetric profile data were generated by averaging the least asymmetric coplanar profiles of the most gradually tapered sample (Sample 4 with $\beta = 52.3$ degrees). These data were then fitted by the same polynomial spline-fitting routine used earlier[1] to simulate a symmetric version of the original sample as shown in Fig. 1a. There, β is the angle between an axial ray and the outer normal to the profile at the inflection point I. Taking the slope of the outer normal as dx/dy, then

$$\beta = -\arctan dx/dy|_I ,$$

where x is the axial location parameter and y is the radial location parameter. The magnitude and location of the derivative at the inflection point are determined from the spline-fitting routine.

It is worth comparing the calculated values of the caustic half-angles for the symmetric melt zone assuming $n = 1.46$ and the corresponding angles originally reported in Ref. 1. For example, the symmetric 2-intercept caustic half-angle, $\theta_A^{U_1}$, of 98.2 degrees, compares well with asymmetric half-angles of 86.8 and 104.7 degrees, for an average of 95.7 degrees. Similarly, with the 3-intercept family, the symmetric data give a caustic half-angle, $\theta_A^D = 148.5$ degrees, whereas the half-angles of

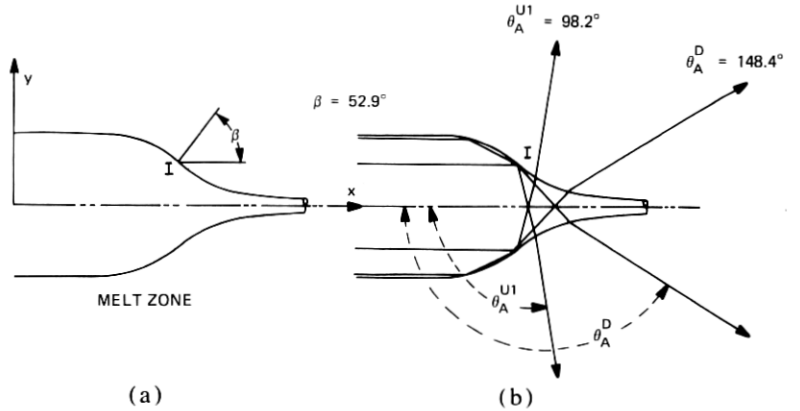

Fig. 1—(a) Symmetric profiles of Sample 4 showing coordinates and inflection point. Here $\beta = 52.92$ degrees, comparable to original data. (b) Symmetric profiles of Sample 4 (as above) showing limiting ray paths for 2-intercept caustics with $\theta_A^{U1} = 98.2$ degrees and for 3-intercept caustics with $\theta_A^{D} = 148.5$ degrees.

138.1 and 154.5 degrees yield an average of 146.3 degrees from the original unsymmetric data.*

The effects of changes in the taper of a symmetric melt zone were revealed by stretching one of the data coordinates by a scale factor before each calculation. With this procedure, increasing the scale factor produces an increase in β and hence a more gradually tapered melt zone. Conversely, decreasing the scale factor decreases β and increases the taper. The slope of the outer normal, dx/dy, at any point on the profile clearly varies linearly with the scale factor.

To quantitatively determine the caustic half-angle, θ_A, as a function of geometry over the maximum possible range, over 130 differently scaled melt zones were analyzed. To establish the generality of these results, the analysis was repeated using data derived from the least symmetric and most sharply tapered of the original samples (Sample 3 with $\beta \simeq 27.5$ degrees).

III. THE CAUSTICS

The two principal families of caustics are of primary interest because they appear over the greatest range of tapers. The first of these caustics is formed by light which reflects internally from a given side, crosses the axis of the melt zone, and is refracted out of the opposite side as shown in Fig. 1b. The second caustic family is due to light which makes two reflections on the initial side, then crosses the axis and is refracted out of the opposite side, as also shown in Fig. 1b. Hereafter, these first

* All angles are measured from the upstream axial direction (see Fig. 1b), whereas in Ref. 1 caustic half-angles for the 3-intercept family were measured from the opposite direction.

and second caustic families will be referred to as "2-intercept" and "3-intercept," respectively.*

Two caustics of lesser interest are also briefly discussed later in this report. The first of these is a "1-intercept" caustic which, as its name implies, is refracted from the glass on its first interception with the surface. The second arises from light which, like the 3-intercept family, reflects twice from the first side before crossing the sample. However, its interception with the opposite side results in an initial reflection and it then refracts from the glass upon its second interception with that side. This is referred to as a "4-intercept" caustic.

Figure 2 presents a plot of the rays which are refracted from the drawdown zone in a sample with $\beta = 69.3$ degrees when 2-intercept light only is emitted. Illuminating rays propagating at greater radial distances than ray 1 or lesser radial distances than ray 3 intercept the second side at angles greater than the critical angle.† Consequently, they are continuously internally reflected and propagate on down the fiber. All the rays between bounding rays 1 and 3 refract out. Ray 2 represents that ray which is incident at the point of maximum slope (labeled *I* in Fig. 2) and is therefore turned through the greatest angle. That ray consequently forms a catacaustic, i.e., a caustic by reflection, within the glass. This caustic travels across the melt zone and forms a visible external caustic when refracted out on the opposite side. From Fig. 2 we see that rays originating on either side of ray 2 are refracted out at angles greater than the ray initially incident at the inflection point.

It should be observed in Fig. 2 that the rays between 1 and 3 which are initially distributed evenly become concentrated near the caustic ray

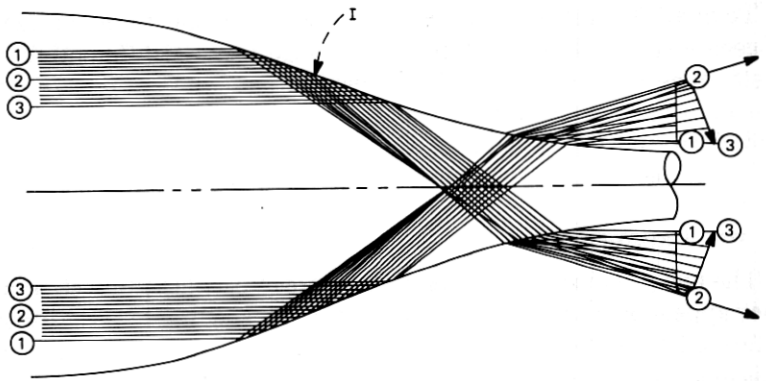

Fig. 2—Symmetric profiles of Sample 4 scaled to give only 2-intercept caustics. The figure shows all trajectories for rays refracting out of the sample between bounding rays 1 and 3 on either side of limiting caustic ray 2. Here $\beta = 69.3$ degrees.

* In Ref. 1, these were referred to as "upstream" and "downstream" caustics because this described their far-field propagation directions as observed in the first of the four original samples studied experimentally.

† Taken as 43.2 degrees, assuming an index of refraction of 1.46 (at the reference wavelength) for fused silica.

as it develops. This concentration of rays symbolizes the intensification of light found along the far-field caustic loci associated with ray 2. Conversely, the rays become widely separated as the bounding rays 1 and 3 are approached, representing a decrease in intensity.

It will be seen that, as β decreases, other 2-intercept caustics appear which are not associated with the internal catacaustic formed at the inflection point. These are due to the refraction of an internal fan of light initially produced by reflection. When the final refraction causes the light to gather into a caustic, it is called a diacaustic.

The 3-intercept caustics also involve an internal catacaustic, due to the interplay between the two initial reflections rather than from the inflection point. In this case, the internal caustic rays originate from rays propagating near the surface of the sample and finally emerge as the far-field caustic rays after refraction. To the best of our understanding, no other 3-intercept rays form externally visible caustics in symmetric melt zones of homogeneous glass.

IV. RESULTS

This section describes the development of the caustic field as a function of the melt zone geometry for the fourth sample. The history of Sample 3 is similar. The reader who is not interested in specific details should proceed to Section V.

We begin by considering melt zone examples with gradual tapers that emit little light and a single caustic. By systematically increasing the taper, we observe an increase in the amount of light emitted and corresponding increases in the number and complexity of the associated caustics. We interpret these results to give the reader a detailed understanding of their significance.

Figure 2 shows a typical distribution of rays throughout the sample including the caustic and bounding ray trajectories. Hereafter, for clarity, we show only the limiting rays (i.e., caustic and bounding rays). However, the reader is reminded that the ultimate intensity distribution is always nonuniform, being much brighter at a caustic and decaying severely as an extinction (e.g., by internal reflection) boundary is approached. Further simplification is effected by separating the graphical information as follows: The melt zone profile and the internal and external caustic rays as they appear are shown in Fig. 3. No other rays are shown. Figures 4 and 5 are "polar plots" of all the far-field limiting rays, for the 2-intercept and 3-intercept families, respectively. The scales are greatly magnified so that the collimated beam is represented as a single horizontal arrow propagating from left to right, and the sample profile is represented as a point. The far-field caustic rays are shown as solid lines and the bounding rays as broken lines. The circumferential arrows follow the continuous fan of light from the outermost bounding ray to the innermost bounding ray, including all caustic rays.

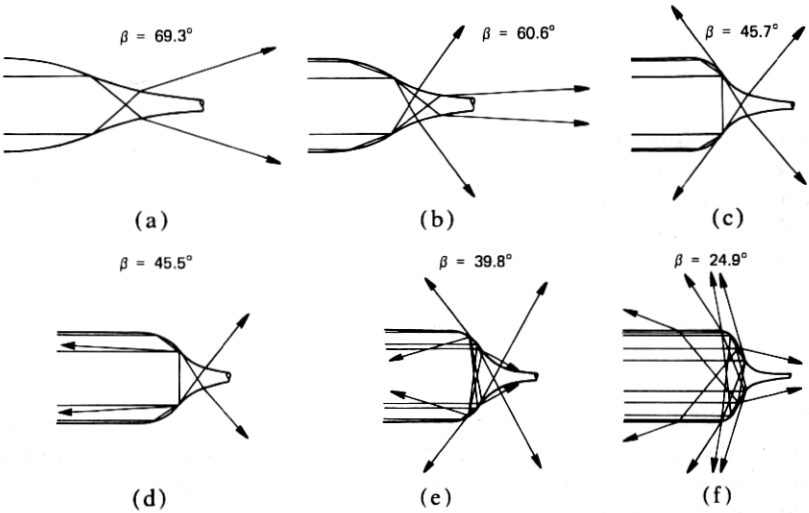

Fig. 3—Symmetric profiles of Sample 4 showing internal and external ray paths for the limiting caustic rays as they appear. (a) $\beta = 69.3$ degrees. Only one 2-intercept caustic is present. (b) $\beta = 60.6$ degrees. Both 2- and 3-intercept caustics are present. (c) $\beta = 45.7$ degrees. Both 2- and 3-intercept caustics are present. (d) $\beta = 45.5$ degrees. Only the 3-intercept caustic is present. (e) $\beta = 39.8$ degrees. 1-, 2-, and 3-intercept caustics are present. (f) $\beta = 24.9$ degrees. 1-, multiple 2-, and 3-intercept caustics are present.

In Fig. 4, the 2-intercept rays are numbered sequentially beginning with the outermost ray 1, which originates near the surface, and increasing inward. The highest numbered ray represents that which initially propagates nearest the sample core and ultimately refracts out.* The 3-intercept rays are lettered *A* through *C* or *D*, as shown in Fig. 5. Each of Figs. 3, 4, and 5 are repeated for a succession of scaled profiles, as shown. The complete range covered in this investigation extends from $\beta = 72$ to $\beta = 6.8$ degrees. In Ref. 1, the corresponding range extended from 53 to about 31.3 degrees.

Figure 3a is the same as Fig. 2, but with the bounding and intermediate rays omitted. The corresponding far-field caustic and bounding ray trajectories are shown in Fig. 4a for the 2-intercept family and Fig. 5a for the 3-intercept family (where the light simply propagates along the sample). Figure 3b shows the emergence of the 3-intercept caustic and a partially rotated 2-intercept caustic. (See also Figs. 4b and 5b.) The 2-intercept caustic originates at the inflection point, as it always must, while the 3-intercept ray originates from a point close to the initial change in the sample cross section, as reported in Ref. 1.

As β continues to decrease, both caustics rotate in an upstream di-

* Actually, of course, the light is not made up of discrete rays but comprises a continuum, including rays on either side of the limiting rays shown. Because of the concentration of rays at the caustic, discreteness errors made in identifying the caustic angles are very small, while those associated with locating the extinction boundaries are substantially larger. The ray spacing used in the present study was optimized so that the caustic angles could be located within +0.1 degree, while the bounding rays are accurate to within no better than ±4 degrees.

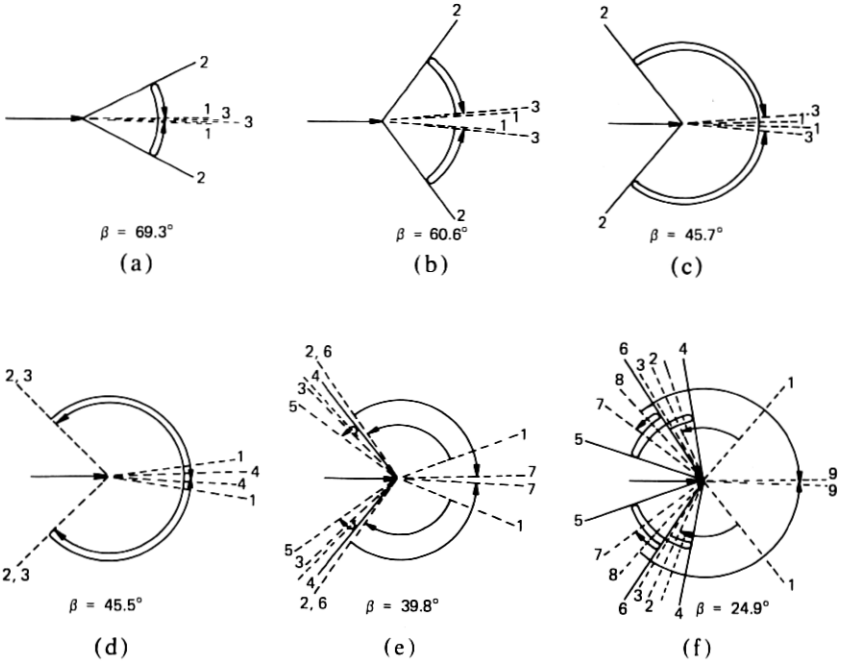

Fig. 4—Schematic diagram showing the external limiting rays for the 2-intercept light paths. The symmetric profiles are omitted, but the orientation is the same as in Fig. 3. The horizontal arrow represents the incoming beam of collimated light illuminating the sample which in turn deflects the light into the plotted ray paths in the far field. Here, the solid lines represent caustics and the broken lines represent bounding rays limited by internal reflection. The circumferential arrows follow the continuous fan of light from the outermost bounding ray to the innermost bounding ray including all caustic limiting rays. The rays are numbered in sequence beginning with 1 as the outermost ray, which originates nearest the surface, and increasing inward. The unnumbered ray in Figs. 4e and 4f represent the last ray after ray 3 which is fully reflected on its first interception with the profiles (except the last two rays, which are again fully reflected). Figures 4a through 4f relate to the same geometrical parameters as Figs. 3a through 3f.

rection, or opposite the rotation of the outer normal at I. Figures 3b and 3c show this rotation quite clearly. Simultaneously, the fans of light forming both caustics broaden (see Figs. 4b and c and 5b and c). However, there is an important distinction between these caustics which may be seen by comparing any two, e.g., Fig. 4c with Fig. 5c. The 2-intercept fan angle is larger and "evenly developed" about the caustic. That is, in Fig. 4c, the fan angle from ray 1 to ray 2 is comparable to the fan angle from ray 2 to ray 3. In contrast, Fig. 5c shows an "unevenly developed" fan of light for the 3-intercept caustic; i.e., the fan angle from ray A to ray B is much greater than the fan angle from ray B to ray C. The reasons for this can be understood by considering how the fans of light are formed internally. The rays forming the 2-intercept caustics are bounded by rays 1 and 3 defined by the internal reflection conditions on the second incident side (see Fig. 2), and therefore give rise to an evenly developed fan. Hereafter, we shall refer to these bounding rays as extinction rays

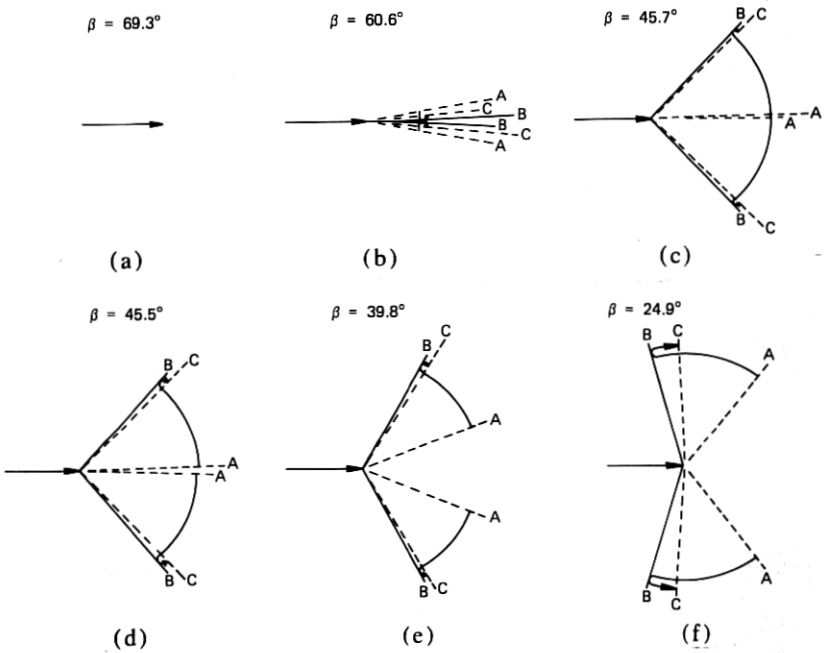

Fig. 5—Schematic diagram showing limiting rays for the 3-intercept light paths. Figure 5 is otherwise the same as Fig. 4, except that the ray sequence is lettered rather than numbered.

because the internal reflection causes extinction of the corresponding external illumination. However, for the 3-intercept family only the outermost bounding ray, A, is an extinction ray defined by the reflection condition on the second side. In contrast, the innermost bounding ray, C, is determined by the presence of the inflection point, which limits the distribution of possible double reflections. In other words, ray C is not an extinction ray as are rays 1, 3, and A, but rather C is a bounding ray determined by the geometrical conditions required for double reflections on the first incident side.

Figures 3d and 4d represent a change of only 0.2 degree from the β of Fig. 3c and show the abrupt extinction of the external 2-intercept caustic due to a second incidence angle in excess of the critical angle, 43.2 degrees. In this case, the 2-intercept catacaustic ray is internally reflected back up the sample, as shown. In Fig. 4d, it can be seen that most of the 2-intercept rays are still incident at angles less than the critical angle and therefore are refracted from the glass. However, two separate fans are formed which are bounded by extinction rays on all sides: rays 1 and 2 and rays 3 and 4. At the same time the 3-intercept caustic simply continues to rotate upstream as seen in Figs. 3d and 5d. As the taper is increased further, β reaches the critical angle at a minimum outer normal slope of 0.98, causing most of the light in the catacaustic ray to refract

from the sample on the first intercept. This results in the family of 1-intercept caustics associated with the inflection point mentioned earlier. Since the optical mechanism by which the light is concentrated is refraction, this is also a diacaustic. Initially, the only light emitted is the ray at the inflection point which exits tangent at the surface (at a half-angle of 226.8 degrees) and follows the glass surface downstream. As β increases, the amount of light refracted increases and the caustic ray refracts from the glass at decreasing angles. It is important to note that this caustic half-angle is always greater than 180 degrees; i.e., it is the only caustic that always propagates toward the axis of the sample.

At $\beta = 40.7$ degrees, a new 2-intercept caustic emerges. Here the two fans of light bounded by extinction rays are still present. In addition, there is a small bundle of rays, including a caustic ray lying between them. This caustic is termed a second 2-intercept caustic because it differs considerably from the original 2-intercept caustic, as may be understood from Figs. 3e and 4e. In Fig. 3e, the usual 3-intercept caustic can be seen originating from the outermost illuminating ray. At this point, it refracts out almost normal to the surface of the melt zone. Therefore, it depends only on the geometry of the melt zone and it is nearly independent of the magnitude of the refractive index. The innermost illuminating ray is incident at the inflection point; it gives rise to two caustics: the external diacaustic (the 1-intercept family discussed above) and the catacaustic associated with the original 2-intercept caustic which has now been reflected internally. A new caustic ray is now shown between these illuminating rays. This new ray gives rise to the new 2-intercept caustic heading upstream in Fig. 3e and is designated ray 4 in Fig. 4e. Then one obvious difference between the second 2-intercept caustic and the original 2-intercept caustic is that the second 2-intercept caustic is not generated from the inflection point. Figure 4e illustrates a second difference: namely, that extinction rays 3 and 5 propagate at smaller angles than caustic ray 4, rather than at larger angles as before. Recall, for example, Fig. 4c, where extinction rays 1 and 3 propagate at much larger angles than caustic ray 2. In other words, the new caustic is formed by a folding in the opposite direction.

Simultaneously, the fan of light formed by the 1-intercept caustic broadens as the band of illuminating rays refracting at the first interception broadens. This band is evenly developed about the inflection point ray, or I ray, and has now expanded to include the rays giving rise to the new 2-intercept caustic. Consequently, most of the light from rays forming this caustic has refracted at the first interception as part of the fan of light which forms the 1-intercept caustic; thus, the second 2-intercept caustic is much less intense than the original. When the second 2-intercept caustic first emerges, however, the band of illuminating rays refracting at the first interception was so small that it did not yet include the rays contributing to the new caustic. This is the case

at $\beta = 40.7$ degrees, where this caustic was still relatively intense. The loss of intensity is illustrated in Fig. 4e by an unnumbered ray representing the last one that is fully reflected on its first interception, shown between rays 3 and 4. Referring to fan 3, 4, and 5, the rays between 3 and the unnumbered ray are totally internally reflected on their first interception and are therefore intense. But the rays between the unnumbered ray and ray 4, then continuing to extinction ray 5, all are less intense since much light is lost on their first interception. Note that all other fans of light are totally reflected on the first interception and are also intense.

Concurrently, it was found that the first extinction rays 1 and A rotate away from their original downstream directions as β decreases from 40.7 degrees. This is not the case for final extinction ray 7, while extinction ray C continues to stay close behind the 3-intercept caustic as it also swings upstream.

At $\beta = 37.3$ degrees, the 2-intercept catacaustic ray, partially reflected at the inflection point from the second side, has re-emerged propagating in the upstream direction. At this stage, it does not form an external caustic as it did earlier. This ray, referred to as the "I ray," is not associated with any stationary point in the angular ray distribution and is located in the intermediate fan of rays. Though theoretically originating as a catacaustic limiting ray within the glass, its caustic character is momentarily lost to external observation because of the dominant effects of the severe spread in refraction angles approaching the extinction ray. Beginning with Fig. 4e, this unnumbered I ray appears between extinction ray 3 and the new caustic ray 4, such that both the caustic and the I ray can be expected to be rather less intense. While the 1- and 3-intercept caustics rotate upstream in the directions of smaller θ_As with decreasing βs, the new 2-intercept caustic rotates in the opposite direction—downstream toward greater caustic angles. In addition, its radial position in the illuminating beam has moved farther out from the center of the sample, away from the I ray and toward the illuminating ray for the 3-intercept caustic. This outward displacement of its illuminating ray and its retrograde rotation are two other properties which make the second 2-intercept caustic different from the first.

When β is decreased further to 34.5 degrees, the first 2-intercept caustic reforms from the I ray, along with yet another 2-intercept caustic. The illuminating ray for the newest caustic propagates just inside the I ray and emerges in the far field barely downstream from the re-emergent first 2-intercept caustic ray. Both these rays are of reduced intensity, since they originate within the band of rays which lose most of their light by refraction on the first interception with the boundary. As the taper is decreased still further, a continued folding of this intermediate fan takes place, and the three 2-intercept caustics separate in the far field. The illuminating rays for the second and third 2-intercept caustics move

away from the I ray. At the same time, the illuminating ray for the third caustic moves in toward the surface. The third 2-intercept caustic, like the second, is folded in a direction opposite that of the first 2-intercept caustic and shows an initial rotation toward smaller θ_As.

One additional point should be noted. In Fig. 3e, soon after the second 2-intercept caustic appeared, its point of emergence moves out along the profile with decreasing β and becomes stationary at the "start" of the melt zone, i.e., the location where the sample begins its decrease in cross section. At the same time, it continues retrograde rotation. On the other hand, the first 2-intercept caustic reappeared as soon as the emergent point of the I ray moved downstream to the same point, so that the outer normal angle becomes constant along the surface and the internal catacaustic could emerge intact with only a change in direction. Subsequently, as β is decreased, the point of emergence of the first 2-intercept caustic moves upstream along the sample surface where the diameter is constant, while the emergent points of both the second and third 2-intercept caustics merge together at the start of the melt zone. Ultimately, both the 3-intercept and the first 2-intercept caustics approach extinction by internal reflection, the latter for a second time as its propagation angle approaches 0 degree. Consequently, their rates of rotation seem to accelerate. From $\beta = 24.9$ degrees (Fig. 3f) to $\beta = 22.3$ degrees, both original caustics disappear by internal reflection, leaving only the second and third 2-intercept and the single 1-intercept caustics in the emerging light field. Figure 4f shows the complicated 2-intercept far-field light ray pattern prior to extinction, with many overlaps between the various fans of light contributing to the structure of the observed illumination. Here the first caustic, ray 5, is once again the extreme upstream ray while all other caustics and extinction boundaries are spread out in the light regions behind it. The unnumbered I ray still lies between ray 3 and the second 2-intercept caustic, ray 4, such that all of the 2-intercept caustics may appear relatively less intense than either the 1- or 3-intercept caustics. At this point, the third 2-intercept caustic, ray 6, has reversed its initial upstream rotation and, like the second 2-intercept caustic, assumed a retrograde rotation with changing slope. In Fig. 5f, $\beta = 24.9$ degrees, the fans of light behind the 3-intercept caustic can be seen to start to broaden slightly just prior to the disappearance of this caustic, while by $\beta = 22.3$ degrees the caustic ray is internally reflected and only the overlapping fans, bounded by extinction boundary rays, and the one geometrical boundary ray, remain. The two remaining 2-intercept caustics (with the original caustic extinguished) continue to rotate toward the downstream direction.

At this geometry, we have probably passed beyond the practical limit for most melt zone profiles drawn in a laser furnace. However, if it were possible to draw even blunter profiles, we would observe that the second 2-intercept caustic angle would approach 90 degrees while the 1-intercept

caustic angle would approach 180 degrees. At the same time, the internally reflected 3-intercept caustic would reappear, at $\beta \cong 16.4$ degrees, although somewhat altered. That is, following the two reflections on the first side of the sample and the initial reflection on the second side, the family forms an internal catacaustic which refracts out of the sample on its next interception with the second side. Since this is a fourth interception overall, it represents the emergence of a 4-intercept caustic rather than a re-emergence of the original 3-intercept caustic. Further blunting of the profile causes the caustic to rotate in the retrograde direction to a maximum caustic half-angle of about 50 degrees, somewhere between $\beta = 14.0$ and $\beta = 13.4$ degrees. It then reverses direction and disappears once more by internal reflection, at $\beta = 6.8$ degrees, leaving only the 1-intercept caustic, which would be very bright, and the second and third 2-intercept caustics, the first of which would also have become bright. Intensification of the light associated with the second 2-intercept caustic results from the outward migration of the associated illumination ray. It eventually reaches a point so near the start of the melt zone surface as to fall incident on the now rapidly curving profile at an angle greater than the critical angle. Consequently it is wholly reflected and all its light is transmitted across the sample to refract out and form the caustic.

V. SUMMARY

The variations of the angles of various 1-, 2-, and 3-intercept caustics as functions of β for both Sample 4 and Sample 3 are given in Figs. 6a and 6b. Significant values are also listed in Table I. In this study, we have identified two additional 2-intercept caustics. Comparison of Figs. 6a and 6b and the tabulated results show that, with the exception of these two caustics, the results for the morphologically different samples are numerically quite similar. Figure 6 also offers a comparison with the results of the original study.[1] For all four samples, these results compare very favorably. Since in Fig. 6 we are comparing results from symmetric samples with the average values obtained from often rather unsymmetric samples, this agreement is quite remarkable.* It is worth noting that in Ref. 1 both the experiments and the original analysis identified only two 2-intercept caustics for Sample 3. In fact, there are three such caustics present. The taper of Sample 3 was such that the first and third 2-intercept caustics were barely separated and consequently appeared to the observer as one.

Turning to the more general results, we see that, for a shallow taper, no light emerges. When β falls below 73 degrees, the 2-intercept caustic emerges, initially directed downstream toward the x-axis and along the surface at an angle, $\theta_A \simeq 190$ degrees. As the taper becomes steeper

* It indicates that, while melt zone asymmetry may have a strong influence on caustic asymmetry, it may have relatively little influence on determining the total caustic cone angle, $2\theta_A$.

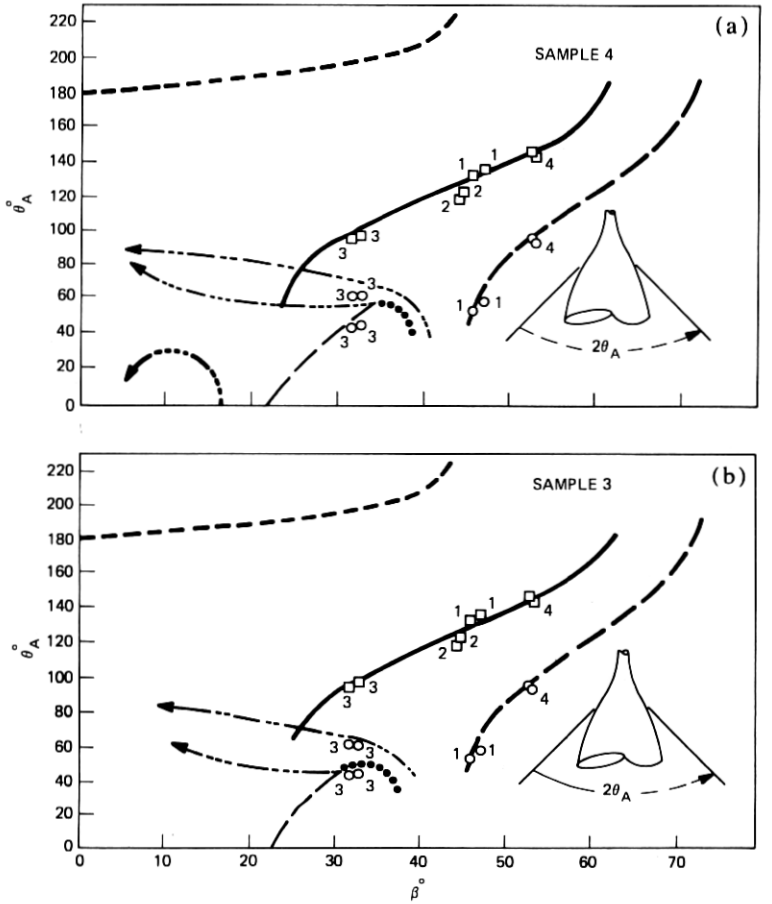

CAUSTIC ANGLE, θ_A, VS. INFLECTION POINT ANGLE, β

- SINGLE INTERCEPT CAUSTIC
- DOUBLE INTERCEPT CAUSTIC
- SECOND DOUBLE INTERCEPT CAUSTIC
- THIRD DOUBLE INTERCEPT CAUSTIC
- TRIPLE INTERCEPT CAUSTIC
- QUADRUPLE INTERCEPT CAUSTIC
- I-RAY ALONE
- [R] DOWNSTREAM DATA, SAMPLE R
- (R) UPSTREAM DATA, SAMPLE R

Fig. 6—Plots of the limiting caustic half-angle, θ_A, vs the angle of the outer normal at the inflection point, β. (a) For symmetric Sample 4. (b) For symmetric Sample 3. The numbered data points represent averaged values of the caustic angles measured on the four original samples described in the earlier study (Ref. 1). Heavy lines denote bright caustic; light lines denote dim caustic.

(β decreases), the caustic ray swings toward the upstream direction. It reaches a half-angle, θ_A, normal to the surface at $\beta \simeq 58$ degrees and a $\theta_A = 90$ degrees at a $\beta \simeq 51$ degrees. Thereafter, its rate of rotation accelerates as it approaches extinction at $\theta_A \simeq 52$ degrees or $\beta \simeq 45.7$ degrees. Recalling that this caustic is the one formed at the inflection point,

Table I—Significant values of limiting caustic half angle

Station \ Caustic Sample Function	2-Intercept				3-Intercept			
	4		3		4		3	
	$\beta°$	$\theta_A^{U1°}$	$\beta°$	$\theta_A^{U1°}$	$\beta°$	$\theta_A^{D°}$	$\beta°$	$\theta_A^{D°}$
At Maximum β	71.7	189.6	72.7	188.5	61.3	186.7	62.6	184.0
At $\theta_A \perp$ Surface	58.5	118.9	58.0	115.0	38.5	116.0	41.6	120.0
At $\theta_A \perp$ X-Axis	51.0	90.0	51.2	90.0	28.4	90.0	29.8	90.0
At Minimum β	45.7	51.9	45.8	52.3	23.7	55.2	25.7	67.2
	2-Intercept				Third 2-Intercept			
	4		3		4		3	
	$\beta°$	$\theta_A^{U1°}$	$\beta°$	$\theta_A^{U1°}$	$\beta°$	$\theta_A^{U3°}$	$\beta°$	$\theta_A^{U3°}$
At Maximum β	34.5	58.5	31.0	46.5	34.5	58.5	31.0	46.5
At Minimum θ_A	23.4	0.0	22.8	0.0	29.6	55.5	26.9	45.3
At Minimum β	23.4	0.0	22.8	0.0	(0.0)*	(90.0)	(0.0)	(90.0)
	Second 2-Intercept				1-Intercept			
	4		3		4		3	
	$\beta°$	$\theta_A^{U2°}$	$\beta°$	$\theta_A^{U2°}$	$\beta°$	$\theta_A^{1°}$	$\beta°$	$\theta_A^{1°}$
At Maximum β	40.7	40.0	38.4	48.0	43.2	226.8	43.2	226.8
At Minimum β	(0.0)	(90.0)	(0.0)	(90.0)	0.0	180.0	0.0	180.0

* Numbers in parentheses were extrapolated and not actually calculated.

it should be noted that, at $\beta \simeq 37.5$ degrees, the internal catacaustic ray, or I ray, again emerges. However, it is not seen as an external caustic until $\beta < 34$ degrees. A different 2-intercept caustic does become visible when $\beta \simeq 40$ degrees. This caustic is not associated with the internal caustic formed by reflection at the inflection point. It also differs from the original 2-intercept caustic in that, as the taper increases, it rotates in the opposite direction, i.e., toward greater angles. It may also emerge initially as an intense caustic, but it becomes quite dim once the incidence angle of the illuminating beam falls below the critical angle. When $\beta < 16.7$ degrees, this new caustic ray is again illuminated by a ray initially at an angle greater than the critical angle and so it again becomes bright. The half-angle, θ_A, of this caustic approaches 90 degrees asymptotically as $\beta \rightarrow 0$ degree. Referring again to the I ray, we see that its rotation is also initially retrograde as β decreases. However, when it again becomes the leading 2-intercept caustic ray, its direction of rotation reverses. From this point, until its extinction at $\beta \simeq 23$ degrees, the reemergent 2-intercept caustic is much less intense. Simultaneously, a third, dim, 2-intercept caustic appears which ultimately rotates in the direction of increasing caustic angle, like the second 2-intercept caustic that preceded it.

Careful study of Figs. 6a and 6b and Table I shows that over most of its range above $\beta = 46$ degrees the 2-intercept caustic θ_A vs β relationship is very nearly the same for both samples. However, this is not true of the second and third 2-intercept caustics, which differ from the first in a number of significant ways. First, the far-field ray trajectories fold in opposite directions. Second, both new caustics rotate to larger rather than smaller caustic angles with decreasing β. Third, they are independent of the internal catacaustic originating at the inflection point. This

latter observation is significant, because while the functional forms of both samples are similar, the additional caustics are quantitatively the most highly differentiated. This differentiability is a result of their originating from rays initially incident far away from the inflection point. There they are more strongly influenced by other aspects of melt zone morphology than just β. More of this will be discussed later in this paper.

The 3-intercept caustic is also less involved with the inflection point and shows some differentiation between the two samples over its entire range (see Table I). Since its initial emergent caustic angle depends on the downstream surface geometry in much the same way as it did for the original 2-intercept caustic, it is not surprising that it too should result in an initial caustic half-angle, θ_A, significantly greater than 180 degrees, although for a 10-degree smaller value of β. As shown in Table I, the final 3-intercept caustic angles are quite different. These extinction angles appear at βs about 22 degrees smaller than their respective 2-intercept caustic's initial extinction β angles and at very nearly the same final extinction β angles as those of the re-emergent first 2-intercept caustic. Actually, the light rays associated with the 3-intercept caustic also eventually make a reappearance. As shown in Fig. 6a for Sample 4, a bright 4-intercept caustic resulting from the internally reflected 3-intercept caustic does emerge briefly headed in the upstream direction and then disappears, all at βs too small to be physically significant.

There is a diacaustic which emerges when β falls below the critical angle. This caustic is formed by the light which refracts from the surface on its first interception. The I ray which forms the internal catacaustic and, ultimately, the 2-intercept caustic, also attains an external extremum when it forms the 1-intercept caustic. Because little of the light in the illuminating rays is reflected, once the 1-intercept caustic appears, many (but not all) of the 2-intercept rays which appear at βs below the critical angle are quite dim. Consequently, over most of this range the 2-intercept caustics are also dim. This is indicated by the light line weights used to represent them in Fig. 6.

While the second and third 2-intercept caustics are unique in that they never propagate downstream or toward the fiber axis, the 1-intercept caustic is also unique because it always propagates downstream toward the fiber axis. Consequently, the 1-intercept caustic either follows the surface or reflects off the fiber at some station downstream, such that its fundamental rotation as a function of β depicted in Fig. 6 becomes reversed. Since this caustic depends only on β, its angle is a unique function of β for all melt zone profiles,

$$\theta_A^1 = 180° - \beta + \arcsin(n \sin \beta),$$

where n is the index of refraction. Hence, for $n = 1.46$ it always originates following the surface downstream at an angle of 226.8 degrees at $\beta = 43.2$ degrees and then rotates toward a limit of 180 degrees.

We conclude that the most useful caustics for studying fiber-drawing melt zones are the first 2-intercept caustic and the 3-intercept caustic. Between them, these cover a broad range of melt zone geometries. Except at very large βs, the first 2-intercept caustic depends mostly on the melt zone profile near the inflection point and does little to distinguish between samples. In contrast, the 3-intercept caustics readily distinguish between the different samples. Sample 3 is on the average larger by about 1.5 degrees in β than Sample 4, a difference originating from variations in geometry near the shoulder and heel of the profiles. Figure 7 presents plots of both sample profiles scaled to a common β of 51.3 degrees. It can be seen that Sample 4 is significantly larger than Sample 3 both upstream, at the shoulder, and downstream, at the heel of the profile. In addition, the inflection point of Sample 4 is at a greater radius, and upstream, of that for Sample 3. Since the β angles are the same, these differences produce a less than 0.7-degree change in the 2-intercept caustic angle θ_A^{U1}. However, the 3-intercept caustic involves reflections at the shoulder region of the melt zone and a refraction at the heel region downstream, and it manifests a change in the caustic angle θ_A^D more than three times that in θ_A^{U1}. As reported in Ref. 1, this difference is detectable experimentally.

Though less intense and of rather limited range, the second and third 2-intercept caustics are also potentially useful as a means of studying melt zone geometries. These are the most distinguishable caustics because they involve light which is initially incident either at the shoulder of the melt zone, as with the second 2-intercept caustic, or at the heel

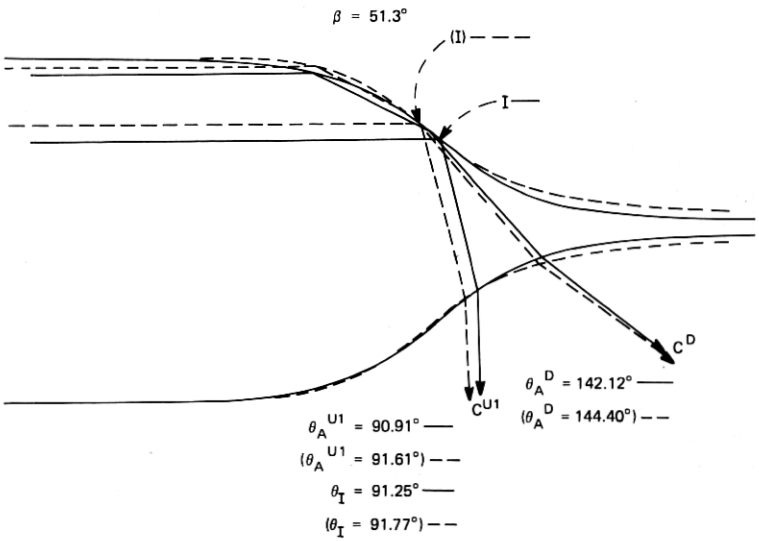

Fig. 7—Superimposed symmetric profiles from Sample 4 (dashed lines) and Sample 3 (solid lines) showing limiting ray paths for both 2- and 3-intercept caustics, one side only. Here, β = 51.3 degrees for both samples with data from Sample 3 shown in parentheses.

of the melt zone as with the third. Both caustics exhibited numerically greater angles for Sample 3 than for Sample 4 whose shoulder and heel profiles induce greater rotations in the reflected rays. Indeed, the averaged experimental results for these caustics from Sample 3 agree reasonably well with the values computed from the symmetric Sample 3 profile data and rather poorly with the values computed from the symmetric Sample 4 profile data, Figs. 6a and 6b, respectively. These caustics are the only primary ones still visible for $\beta < 22$ degrees, and together with the 1-intercept caustic provide some means of studying extremely blunt melt zones.

It should be realized that, since each of these six caustics under discussion involves a refraction from the sample, they all may depend on the index of refraction, n, as well as on the surface geometry. In Ref. 1, another caustic generated wholly by reflection and dependent only on β was discussed. That caustic is the externally illuminated equivalent of the internal catacaustic that forms at the inflection point and can easily be generated for all physically reasonable melt zone profiles. Since it does not depend on n, information from this externally illuminated catacaustic may be used to separate the β dependence of the data obtained from an appropriate internally illuminated caustic. This could provide otherwise unavailable information concerning the index of refraction. For example, consider a melt zone sample of unknown n exhibiting a first 2-intercept caustic at an angle θ_A^{U1} somewhere between 52 and 110 degrees. It may be matched with a computer analysis of the present data at a β determined from direct measurement of the externally illuminated catacaustic angle, θ_A^{EXT}. Adjustment of the n value used in the computer analysis to yield an equal theoretical θ_A^{U1} value should provide a good estimate of the unknown index of refraction. The quality of this estimate would depend on how uniform n was across the sample and how close the propagation vector of the emerging caustic was to tangency with the surface. Obviously, if β is such that the caustic emerges normal to the surface, it can provide no information about n.

VII. ACKNOWLEDGMENT

The authors wish to acknowledge the collaboration of J. McKenna, who contributed to the development of the numerical algorithm.

REFERENCE

1. P. G. Simpkins, T. D. Dudderar, J. McKenna, and J. B. Seery, "On the Occurrence of Caustics in the Drawdown Zone of Silica Fibers," B.S.T.J., *56*, No. 4 (April 1977), pp. 535–560.